Published in final edited form as:
Biochem Biophys Res Commun. 2007 September 7; 360(4): 797–801.

Directional memory and caged dynamics in cytoskeletal remodelling

Guillaume Lenormand[*], **Julien Chopin**, **Predrag Bursac**, **Jeffrey J. Fredberg**, and **James P. Butler.**
Molecular and Integrative Physiological Sciences, Department of Environmental Health, School of Public Health, Harvard University, Boston, MA, USA

Abstract

We report directional memory of spontaneous nanoscale displacements of an individual bead firmly anchored to the cytoskeleton of a living cell. A novel method of analysis shows that for shorter time intervals cytoskeletal displacements are antipersistent and thus provides direct evidence in a living cell of molecular trapping and caged dynamics. At longer time intervals displacements are persistent. The transition from antipersistence to persistence is indicative of a time-scale for cage rearrangements and is found to depend upon energy release due to ATP hydrolysis and proximity to a glass transition. Anomalous diffusion is known to imply memory, but we show here that memory is attributed to direction rather than step size. As such, these data are the first to provide a molecular-scale physical picture describing the cytoskeletal remodelling process and its rate of progression.

Keywords

Magnetic twisting cytometry; soft glassy rheology; jamming; spontaneous bead motion; actin dynamics; human airway smooth muscle

INTRODUCTION

The network of biopolymers that confers shape stability and mechanical integrity to the living cell is called the cytoskeleton (CSK). The CSK is highly dynamic and in a constant state of remodelling. This CSK remodelling, in turn, is fundamental to a wide variety of cellular functions including locomotion, invasion, contraction, and wound healing, but the physical laws governing underlying molecular-scale structural rearrangements within the CSK remain quite unclear. Recently we have reported a striking but controversial analogy between the dynamics of the CSK and that of inert out-of-equilibrium systems, especially soft glassy materials [1;2;3;4;5]. From forced motions of a microbead tightly bound to the CSK of the living cell, we established scale-free rheology [4;5], mechanical aging [1], and shear-induced fluidization [1;2], and from spontaneous nanoscale motions of the same bead we established intermittent dynamics, slow relaxation, approach to kinetic arrest, and breakdown of the fluctuation-dissipation theorem [1;2]. These out-of-equilibrium dynamics, taken together, are strongly reminiscent of those that are characteristic of inert soft glassy materials [6].

* Corresponding author: Dr. Guillaume Lenormand, Molecular and Integrative Physiological Sciences, Department of Environmental Health, School of Public Health, Harvard University, 665 Huntington Avenue, Bldg I, room 1305, Boston, MA 02115, USA, Phone: 617 432 1477, Fax: 617 432 4710, E-mail: glenorma@hsph.harvard.edu.

Nonetheless, the extent to which the CSK properly belongs to the class of soft glassy materials remains a question of some debate [7;8;9]. In a soft glassy material, slow relaxation and approach to kinetic arrest are thought to reflect approach to a glass transition and associated confinement of a constitutive particle by a cage formed by its neighbours [6;10;11]. It is the structural rearrangement of this cage that is thought to lead to the final slow structural relaxation that limits the rate of particle diffusion through the sample.

Caged dynamics have been suggested in the past based upon observations of the mean square displacement, $<r^2(t)>$, of sequential tracer displacements during anomalous diffusion [1;10; 11], but because the mean square displacement cannot distinguish between memory of tracer step size versus memory of step direction, that measure of anomalous diffusion is merely suggestive of caged motion (online supplement 1). Based upon correlations of tracer sequential angular displacements, by contrast, we report here the first direct evidence of directional memory and caged dynamics at the molecular level. At short time intervals, Δt, displacements are found to be antipersistent; when a step is in one direction, the following step is more likely to be in the opposite direction, and therefore this behaviour provides the first direct evidence of molecular trapping and caged dynamics. At longer Δt, however, displacements are found to be persistent; when a step is in one direction, the following step is more likely to be in the same direction.

MATERIALS AND METHODS

Microbead coating, cell preparation, and mean square displacement measurements used in this paper are described in detail elsewhere [1;12;13] and are summarized below.

Microbead and living cell preparation

Ferrimagnetic microbeads (4.2 μm in diameter) are produced in our laboratory, and coated with a peptide containing the sequence Arg-Gly-Asp (150 μg ligand/mg microbeads) by overnight incubation at 4°C in carbonate buffer (pH 9.4). Human airway smooth muscle (HASM) cells in passage 6–7 are serum-deprived for 24 h; serum deprivation arrests the cell cycle in the G_1/G_0 phases. Plastic wells (6.4 mm, 96-well Removawells, Immunlon, IL) are coated with collagen I at a density of 500 ng/cm^2 for at least 12 hrs. Cells are harvested with trypsin and incubated overnight in collagen-coated wells at confluence (~20,000 cells/well). Prior to each measurement, approximately 10,000 microbeads are added to an individual well and incubated for 20 min. The well is then rinsed twice with serum-free medium at room temperature to remove unbound microbeads.

Reagents

Tissue culture reagents are obtained from Sigma (St. Louis, MO, USA), with the following exceptions: Trypsin-ETDA solution, which is purchased from Gibco (Grand Island, NY), Type I rat tail collagen (Vitrogen Collagen) from Cohesion Technologies (Palo Alto, CA), RGD peptide (Peptide 2000) from Telios Pharmaceuticals (San Diego, CA), jasplakinolide from CalBiochem (La Holla, CA). Jasplakinolide (Jasp) and cytochalasin-D are prepared in sterile dimethylsulfoxide (DMSO). Histamine and dibutyryl adenosine 3′,5′-cyclic monophosphate (DBcAMP) are reconstituted in sterile distilled water. On the day of experiments, all drugs are diluted to final concentrations in serum-free media, yielding less than 0.1% DMSO in final volume.

ATP is depleted by incubation with 2 mM deoxyglucose and 2 mM NaN_3. Residual ATP is assayed using a standard luciferase-based ATP determination kit (Sigma), and concentrations after depletion are from 2–7% of that in control samples.

Mean square displacement measurements

When a RGD-coated microbead is incubated on the surface of a HASM cell, it ligates integrin receptors and forms focal adhesion complexes. Mechanical responses of such a bead have a precise locus that remains equivocal [9;14;15;16;17], but these responses have been shown in an unequivocal manner to be highly sensitive to manipulations of actin filaments, myosin motors, vinculin, heat shock proteins 20 and 27, cell spreading, cell stretching, cytoskeletal tension, and depletion of ATP [1;2;4;18;19;20;21;22;23;24;25]. We reasoned, accordingly, that the bead can move spontaneously only if the cytoskeletal structures to which it is attached rearrange; therefore, spontaneous bead motions report ongoing CSK remodelling in space and time [18], where by CSK we mean any structure or molecule that contributes appreciably to the integrated mechanical properties of the cell.

Spontaneous bead motions are measured by identifying the position of the centre of mass of each bead (approximately 100 beads per field-of-view) at the rate of 12 frames per second (0.082 seconds per frame) at 40× magnification for 5 or 10 min. Bead positions are corrected for the effects of microscope stage drift; the stage drift is estimated from changes in the mean position of all beads within a field of view. We define mean square displacement, $\langle r^2(\Delta t)\rangle$, as $\langle r^2(\Delta t)\rangle = \langle (r(t+\Delta t) - r(t))^2\rangle$, where r(t) is the bead position at time t, Δt is the time lag, and brackets indicate an average over t and over all beads [1;12].

Elastic modulus measurements

To estimate the stiffness of structures bound to the bead, microbeads are first magnetized horizontally (parallel to the surface on which cells were plated) and then twisted in a vertically aligned homogenous magnetic field at different frequencies – from 0.1 to 10^3 Hz. The resulting lateral bead displacements in response to the oscillatory torque are measured optically. The cell elastic modulus, gcc, is defined as the real part in Fourier space of the ratio of specific torque to lateral bead displacements; g′ is expressed in units of Pa/nm.

RESULTS AND DISCUSSION

We begin by quantifying $\langle r^2(\Delta t)\rangle$ on the nanometre scale [1] (online supplement 2). For short Δt, $\langle r^2(\Delta t)\rangle$ increases only modestly with Δt, roughly following a power-law with exponent β significantly less than one (Fig. 1), indicating subdiffusive behaviour. By contrast, for large Δt, $\langle r^2(\Delta t)\rangle$ increases much faster, approximating a power-law with β significantly greater than one, indicating superdiffusive behaviour. The amplitude of $\langle r^2(\Delta t)\rangle$ as well as the transition time from subdiffusive to superdiffusive behaviour depend upon thermodynamic temperature (Fig. 1a), CSK treatments, and ATP depletion (Fig. 1b).

But to what extent is the motion in some particular direction correlated with continued motion in that direction? There are essentially three possible answers to this question. First, changes in direction might be more or less uniformly distributed over all angles θ in $(-\pi, \pi]$, where we denote the change in angular direction of two successive steps by $\theta \in (-\pi, \pi]$. Such an outcome would be interpreted as direct evidence of independence in step increment directionality. Second, changes in direction might be concentrated near $\theta = 0$; this outcome would indicate persistence of motion consistent with superdiffusive behaviour. Third, changes in direction might be concentrated near $|\theta|=\pi$; this outcome would indicate antipersistence in the sense that directional reversals are the more likely realizations of the motion. Such behaviour would in turn be interpreted as direct evidence of caged behaviour.

Accordingly, from the same microbead trajectories used for measuring $\langle r^2(\Delta t)\rangle$, we compute $p(\Delta t, \theta)\, d\theta$, the probability of having θ in the interval $[\theta, \theta + d\theta]$. Figure 2 shows measurements performed at 23°C. For $\Delta t < 0.24$ s, the maximum of $p(\Delta t, \theta)$ is for angles in the vicinity of

$-\pi$ or π (Fig. 2a). On average, each bead displays an antipersistent behaviour; when a step is in one direction, the following step is more likely to be in the opposite direction and thus provides direct evidence of caged motion. For $0.24 < \Delta t < 0.33$ s, $p(\Delta t, \theta)$ approximates the uniform distribution. At longer Δt, the maximum of $p(\Delta t, \pi)$ is in the forward direction, $\theta \sim 0$. On average, each bead displays a persistent behaviour; when a step is in one direction, the following step is more likely to be in the same direction. For $\Delta t > 6.60$ s, $p(\Delta t, \theta)$ still displays a maximum value for $\theta \sim 0$, but the probability of $\theta \sim 0$ is slowly decreasing as Δt increases (Fig. 2b). A similar behaviour is observed for each thermodynamic temperature, each CSK treatment and ATP depletion (data not shown).

The transition from antipersistent to persistent behaviour occurs near the essentially uniform distribution, $u(\theta) = 1/2\pi$ (Fig. 2a). Consequently, to directly measure Δt^* we quantify the departure of $p(\Delta t, \theta)$ from $u(\theta)$ using the Kolmogorov-Smirnov statistical test [26;27]. This test is defined as $KS(\Delta t) = \sqrt{n}\max_{-\pi<\theta\leq\pi} |F(\Delta t, \theta) - U(\theta)|$, where $F(\Delta t, \theta)$ is the observed cumulative distribution function of angles, $U(\theta) = (\theta + \pi)/2\pi$ is the cumulative uniform distribution function, and n is the number of observations. In order to do quantitative comparison between groups, we focus on $K(\Delta t) = KS(\Delta t)/\sqrt{n}$. $K(\Delta t)$ is zero when $p(\Delta t, \theta)$ is a uniform distribution, and 0.5 when $p(\Delta t, \theta)$ is a purely persistent distribution. The time interval at which $K(\Delta t)$ is minimum should, therefore, correspond to the transition time, Δt^*, from antipersistent to persistent behaviour. In most cases, $K(\Delta t)$ first decreases, passes through a sharp minimum, then increases again to a maximum, denoted K_{max}, and decreases at longer time intervals (Fig. 3). However, at 39°C and 41°C, the first minimum presumably occurs before the first measurement at 0.082 s; when ATP is depleted, K_{max} presumably occurs after the last measurement at 60.25 s. Δt^* and K_{max} depend upon thermodynamic temperatures (Fig. 3a), CSK treatments and ATP depletion (Fig. 3b). Empirically, Δt^* is found to correspond to the transition time between subdiffusive and superdiffusive behaviours (Fig. 1 and 2), and is comparable to the time interval at which the non-Gaussian parameter α reaches its peak value [1;10;11]. Therefore Δt^* could be indicative of the time-scale of cage rearrangement.

Direct evidence of caged motion as provided here further strengthens the analogy between CSK dynamics and that of inert out-of-equilibrium systems such as soft glassy materials [1; 3;4;28;29]. A physical picture capturing these dynamics uses an energy landscape to describe microconfigurations of CSK structures [6]. Each CSK structure (*e.g.* structural protein or protein complex) finds itself trapped by interactions with its surrounding neighbours. Because these neighbours act as a cage, particle motions are localized most of the time, although occasionally a particle escapes its trap and thus causes the local microconfiguration to rearrange (remodel). Trapping in such out-of-equilibrium systems arises due to the insufficiency of thermal energy to drive structural rearrangements; this is analogous to a jammed state [30; 31]. Therefore the cage rearrangement time-scale and its increase as the CSK approaches the glass transition – a phenomenon reminiscent of kinetic arrest – become of interest [1;10;11].

To test further the plausibility of this interpretation, we next considered the relationship between directional memory and proximity of the CSK to a glass transition. As shown previously [1;4], over a wide range of frequencies, f, the cell elastic modulus, g', shows a weak power-law dependence on frequency, $g'(f) \sim f^{x-1}$. As $x \rightarrow 1$, the system approaches purely elastic behaviour, and in the theory of soft glassy rheology, the system approaches a glass transition [6]. Therefore we took x as a measure of proximity to a glass transition, and we determined its value from $g'(f)$ (data not shown). As thermodynamic temperatures decreases, x approaches 1 and Δt^* increases (Fig. 4a). Interpreted in this context, the cages become more long-lived as the CSK approaches the glass transition, presumably because cage rearrangements involve a larger number of particles as the glass transition is approached [10; 11;32]. But for CSK manipulations, Δt^* shows a weaker dependence on x and does not seem to be determined solely by x. Note here a kind of paradox in which the power-law behaviour

of g′ has no intrinsic time-scale [4;5] whereas K(Δt) (or $<r^2(\Delta t)>$) shows a particular time-scale. Interestingly as $x \rightarrow 1$, K_{max} increases strongly and in a linear fashion with x (Fig. 4b), a behaviour reminiscent of colloidal systems approaching a glass transition, and indicative of approach to kinetic arrest [10;32]. The linear relation between K_{max} and x does not hold with cytochalasin-D, however, a drug that disrupts actin filaments and thus modifies cytoskeletal structures.

Although dynamics of soft glassy systems are illustrated most simply in a crowded colloidal suspension, similar dynamics can arise from other physical interactions such as attractive interactions or weak chemical bonding. As such, the caged-dynamics reported here could be consistent with force fluctuations arising from the constantly remodelling pre-stressed network of F-actin to which the bead is firmly connected. Finally, we note that data reported here and those of Kusumi and co-workers [33;34] are remarkably similar whereas our respective interpretations are fundamentally different. Kusumi et al. suggest that the trajectory of a very small surface-bound marker is confined to a cage created by a fixed cytoskeletal ‘fence’, whereas here we used markers that are much too large to be confined by any such fence and, accordingly, we attribute our results to dynamics of the CSK itself.

Supplementary Material

Refer to Web version on PubMed Central for supplementary material.

Acknowledgements

We thank Reynold A. Panettieri Jr. for providing HASM cells, and Emil Millet for producing the magnetic beads. This study was supported by National Institute of Health Grant Nos. HL 33009, HL/AI 65960, HL 59682.

References

1. Bursac P, Lenormand G, Fabry B, Oliver M, Weitz DA, Viasnoff V, Butler JP, Fredberg JJ. Cytoskeletal remodelling and slow dynamics in the living cell. Nat Mater 2005;4:557–61. [PubMed: 15937489]
2. Trepat X, Deng L, An SS, Navajas D, Tschumperlin DJ, Butler JP, Gerthoffer WT, Fredberg JJ. Universal physical responses to stretch in the living cell. Nature. 2007in press
3. Deng L, Trepat X, Butler JP, Millet E, Morgan KG, Weitz DA, Fredberg J. Fast and slow dynamics of the cytoskeleton. Nat Mater 2006;5:636–40. [PubMed: 16845421]
4. Fabry B, Maksym GN, Butler JP, Glogauer M, Navajas D, Fredberg JJ. Scaling the microrheology of living cells. Phys Rev Lett 2001;87:148102. [PubMed: 11580676]
5. Lenormand G, Millet E, Fabry B, Butler JP, Fredberg JJ. Linearity and time-scale invariance of the creep function in living cells. J R Soc Interface 2004;1:91. [PubMed: 16849155]
6. Sollich P. Rheological constitutive equation for a model of soft glassy materials. Phys Rev E 1998;58:738–759.
7. Balland M, Desprat N, Icard D, Fereol S, Asnacios A, Browaeys J, Henon S, Gallet F. Power laws in microrheology experiments on living cells: comparative analysis and modelling. Phys Rev E 2006;74:021911.
8. Hoffman BD, Massiera G, Van Citters KM, Crocker JC. The consensus mechanics of cultured mammalian cells. Proc Natl Acad Sci U S A 2006;103:10259–64. [PubMed: 16793927]
9. Van Citters KM, Hoffman BD, Massiera G, Crocker JC. The role of F-actin and myosin in epithelial cell rheology. Biophys J. 2006
10. Weeks ER, Crocker JC, Levitt AC, Schofield A, Weitz DA. Three-dimensional direct imaging of structural relaxation near the colloidal glass transition. Science 2000;287:627–631. [PubMed: 10649991]
11. Weeks ER, Weitz DA. Properties of cage rearrangements observed near the colloidal glass transition. Phys Rev Lett 2002;89:095704. [PubMed: 12190415]

12. Bursac P, Fabry B, Trepat X, Lenormand G, Butler JP, Wang N, Fredberg JJ, An SS. Cytoskeleton dynamics: Fluctuations within the network. Biochem Biophys Res Commun. 2007
13. Fabry B, Maksym GN, Butler JP, Glogauer M, Navajas D, Taback NA, Millet EJ, Fredberg JJ. Time scale and other invariants of integrative mechanical behavior in living cells. Phys Rev E 2003;68:041914.
14. Matthews BD, Overby DR, Alenghat FJ, Karavitis J, Numaguchi Y, Allen PG, Ingber DE. Mechanical properties of individual focal adhesions probed with a magnetic microneedle. Biochem Biophys Res Commun 2004;313:758–64. [PubMed: 14697256]
15. Overby DR, Matthews BD, Alsberg E, Ingber DE. Novel dynamic rheological behavior of individual focal adhesions measured within single cells using electromagnetic pulling cytometry. Acta Biomater 2005;1:295–303. [PubMed: 16701808]
16. Puig-de-Morales M, Millet E, Fabry B, Navajas D, Wang N, Butler JP, Fredberg JJ. Cytoskeletal mechanics in adherent human airway smooth muscle cells: probe specificity and scaling of protein-protein dynamics. Am J Physiol Cell Physiol 2004;287:C643–54. [PubMed: 15175221]
17. Sniadecki NJ, Desai RA, Ruiz SA, Chen CS. Nanotechnology for cell-substrate interactions. Ann Biomed Eng 2006;34:59–74. [PubMed: 16525764]
18. An SS, Fabry B, Mellema M, Bursac P, Gerthoffer WT, Kayyali US, Gaestel M, Shore SA, Fredberg JJ. Role of heat shock protein 27 in cytoskeletal remodeling of the airway smooth muscle cell. J Appl Physiol 2004;96:1701–13. [PubMed: 14729728]
19. An SS, Laudadio RE, Lai J, Rogers RA, Fredberg JJ. Stiffness changes in cultured airway smooth muscle cells. Am J Physiol Cell Physiol 2002;283:C792–801. [PubMed: 12176736]
20. Deng L, Fairbank NJ, Cole DJ, Fredberg JJ, Maksym GN. Airway smooth muscle tone modulates mechanically induced cytoskeletal stiffening and remodeling. J Appl Physiol 2005;99:634–41. [PubMed: 15845778]
21. Laudadio RE, Millet EJ, Fabry B, An SS, Butler JP, Fredberg JJ. Rat airway smooth muscle cell during actin modulation: rheology and glassy dynamics. Am J Physiol Cell Physiol 2005;289:C1388–95. [PubMed: 16120653]
22. Stamenovic D, Suki B, Fabry B, Wang N, Fredberg JJ. Rheology of airway smooth muscle cells is associated with cytoskeletal contractile stress. J Appl Physiol 2004;96:1600–1605. [PubMed: 14707148]
23. Hu S, Chen J, Fabry B, Numaguchi Y, Gouldstone A, Ingber DE, Fredberg JJ, Butler JP, Wang N. Intracellular stress tomography reveals stress focusing and structural anisotropy in cytoskeleton of living cells. Am J Physiol Cell Physiol 2003;285:C1082–C109. [PubMed: 12839836]
24. Wang N, Tolic-Norrelykke IM, Chen J, Mijailovich SM, Butler JP, Fredberg JJ, Stamenovic D. Cell prestress. I. Stiffness and prestress are closely associated in adherent contractile cells. Am J Physiol Cell Physiol 2002;282:C606–C616. [PubMed: 11832346]
25. Ezzell RM, Goldmann WH, Wang N, Parasharama N, Ingber DE. Vinculin promotes cell spreading by mechanically coupling integrins to the cytoskeleton. Exp Cell Res 1997;231:14–26. [PubMed: 9056408]
26. Knuth DE. The art of computer programming. Vol. 2: Seminumerical algorithms. Reading. 1981
27. D.E. Knuth, Seminumerical algorithms, the art of computer programming.
28. Bandyopadhyay R, Liang D, Harden JL, Leheny RL. Slow dynamics, aging, and glassy rheology in soft and living matter. Solid State Communications. 2006
29. Desprat N, Richert A, Simeon J, Asnacios A. Creep function of a single living cell. Biophys J 2005;88:2224–33. [PubMed: 15596508]
30. Liu AJ, Nagel SR. Nonlinear dynamics: Jamming is not just cool any more. Nature 1998;396:21–22.
31. Trappe V, Prasad V, Cipelletti L, Segre PN, Weitz DA. Jamming phase diagram for attractive particles. Nature 2001;411:772–775. [PubMed: 11459050]
32. Kob W, Donati C, Plimpton SJ, Poole PH, Glotzer SC. Dynamical heterogeneities in a supercooled Lennard-Jones liquid. Phys Rev Lett 1997;79:2827–2830.
33. Abbott A. Cell biology: hopping fences. Nature 2005;433:680–3. [PubMed: 15716923]

34. Kusumi A, Sako Y, Yamamoto M. Confined lateral diffusion of membrane receptors as studied by single particle tracking (nanovid microscopy). Effects of calcium-induced differentiation in cultured epithelial cells. Biophys J 1993;65:2021–40. [PubMed: 8298032]

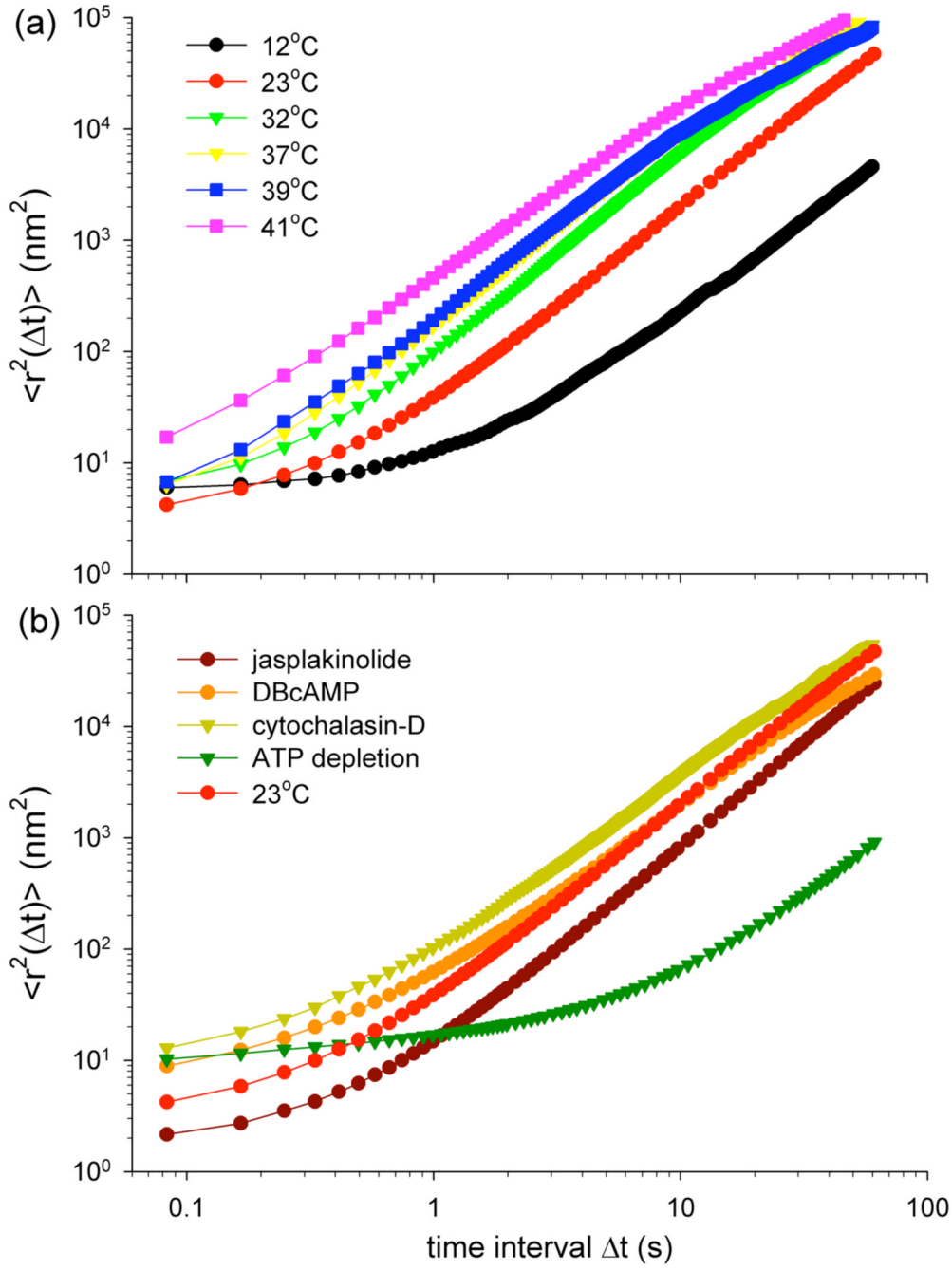

FIG. 1.

Mean square displacements, $\langle r^2(\Delta t)\rangle$, computed from spontaneous motion of RGD-coated beads (400 to 720 beads per group). (a) $\langle r^2(\Delta t)\rangle$ at different thermodynamic temperatures, from 12°C to 41°C. (b) $\langle r^2(\Delta t)\rangle$ under baseline condition (23°C), and after challenge with DBcAMP (decreases cell contractility, 1 mM), jasplakinolide (stabilizes actin, 1 μM), cytochalasin-D (disrupts actin filaments, 2 μM), and after depleting ATP. ATP concentration after depletion was from 2 to 7% of that in control samples. Noise level on bead position is discussed in Bursac et al.[1] and in Online Supplement 2.

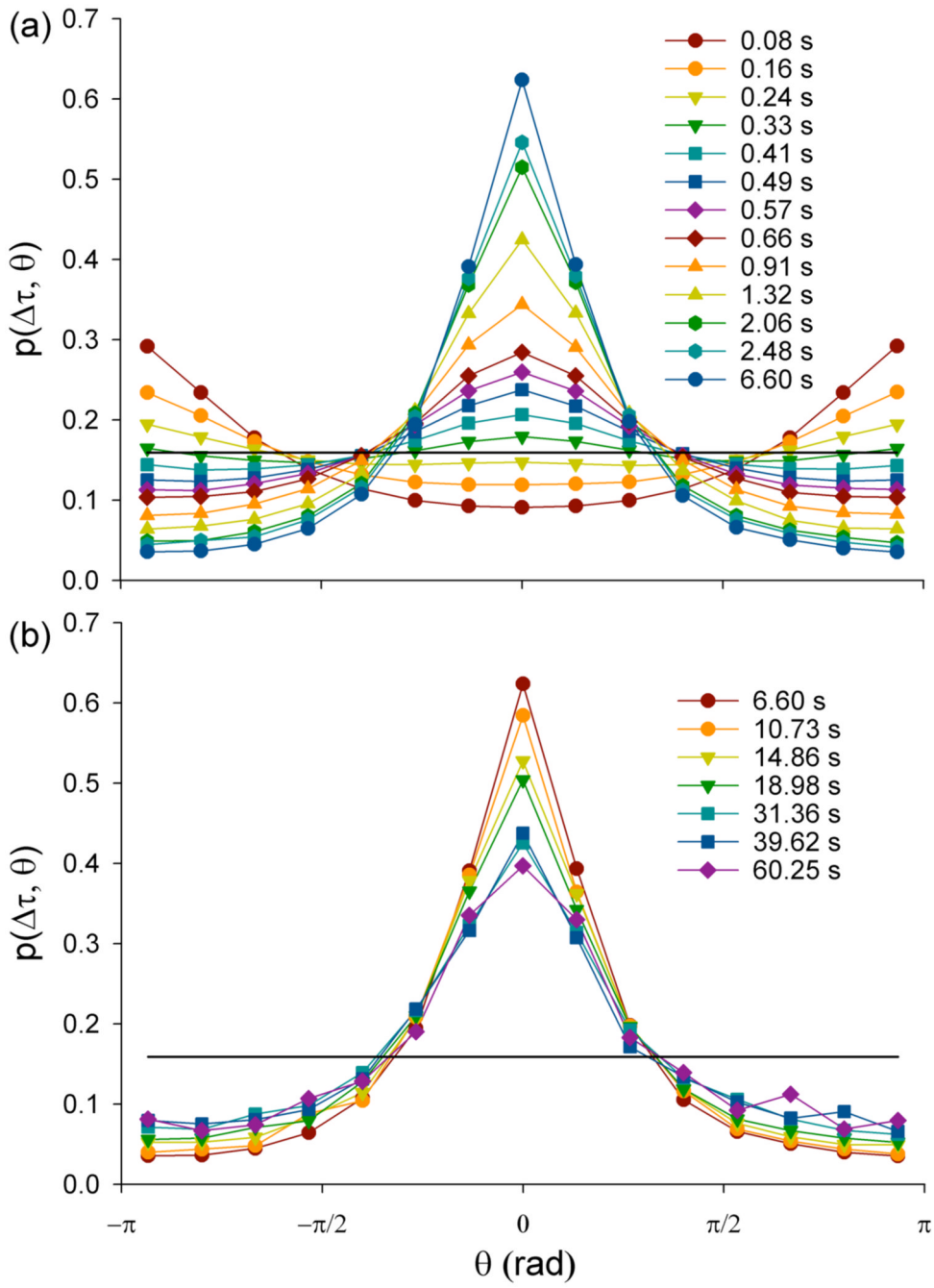

FIG. 2.

Probability density functions of angles, p(Δt,θ), for baseline condition (23°C) at different time intervals Δt, (a) from 0.08 s to 6.60 s and (b) from 6.60 s to 60.25 s. p(Δt,θ) is computed from the same bead trajectories as $\langle r^2(\Delta t)\rangle$ (Fig. 1), averaging over 428 beads, yielding from 1.7×10^6 events at Δt = 0.082 s down to 1.3×10^3 events at Δt = 60.25 s. When averaging, time intervals do not overlap in order to avoid artifactual correlations between angles. Bin size is 2π/15. Solid line is uniform distribution u(θ) = 1/2π.

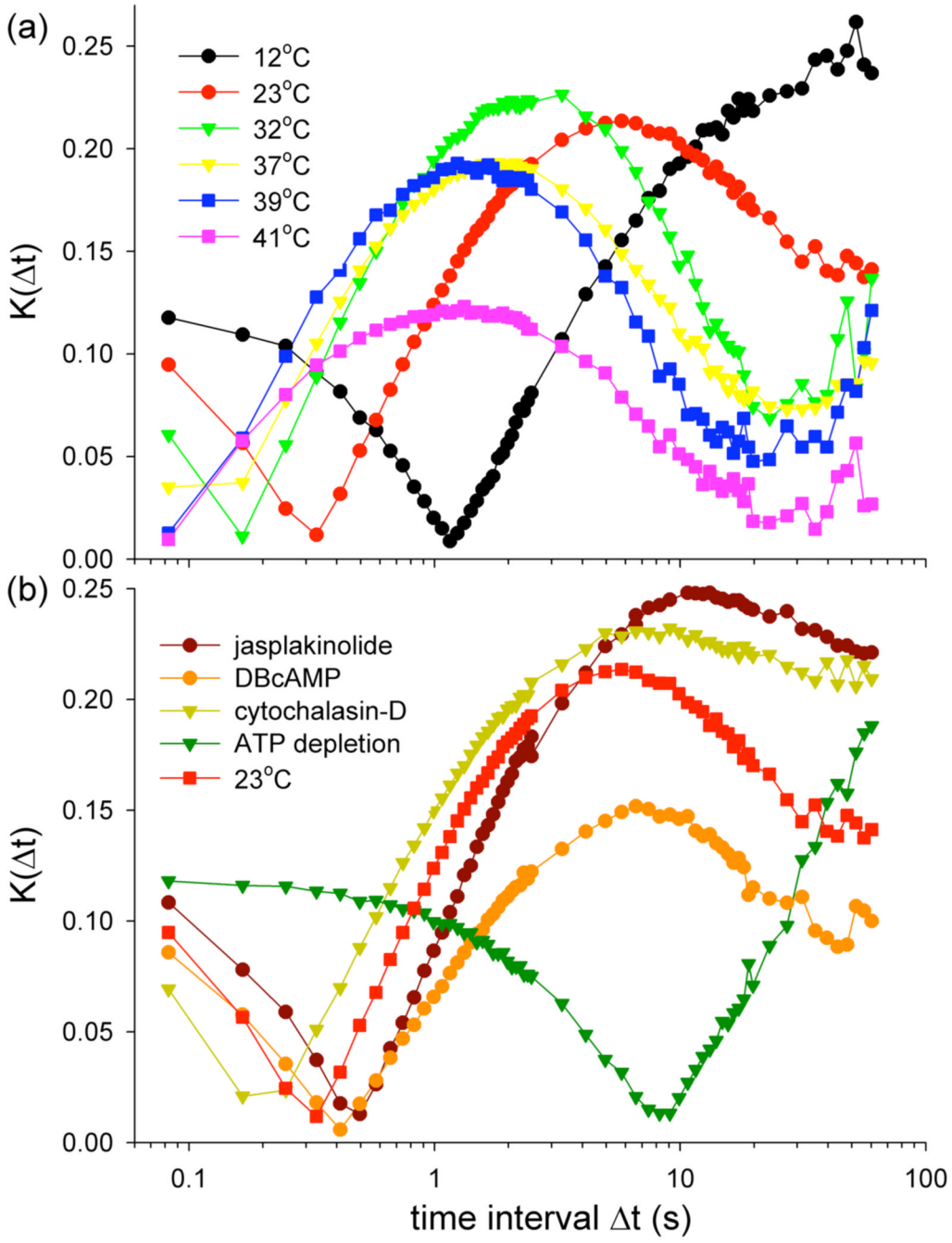

FIG. 3.

The departure of p(Δt,θ) from a uniform distribution is quantified using the Kolmogorov-Smornov statistical test, K(Δt), (a) at different thermal temperatures, and (b) with different CSK treatments, and after ATP depletion.

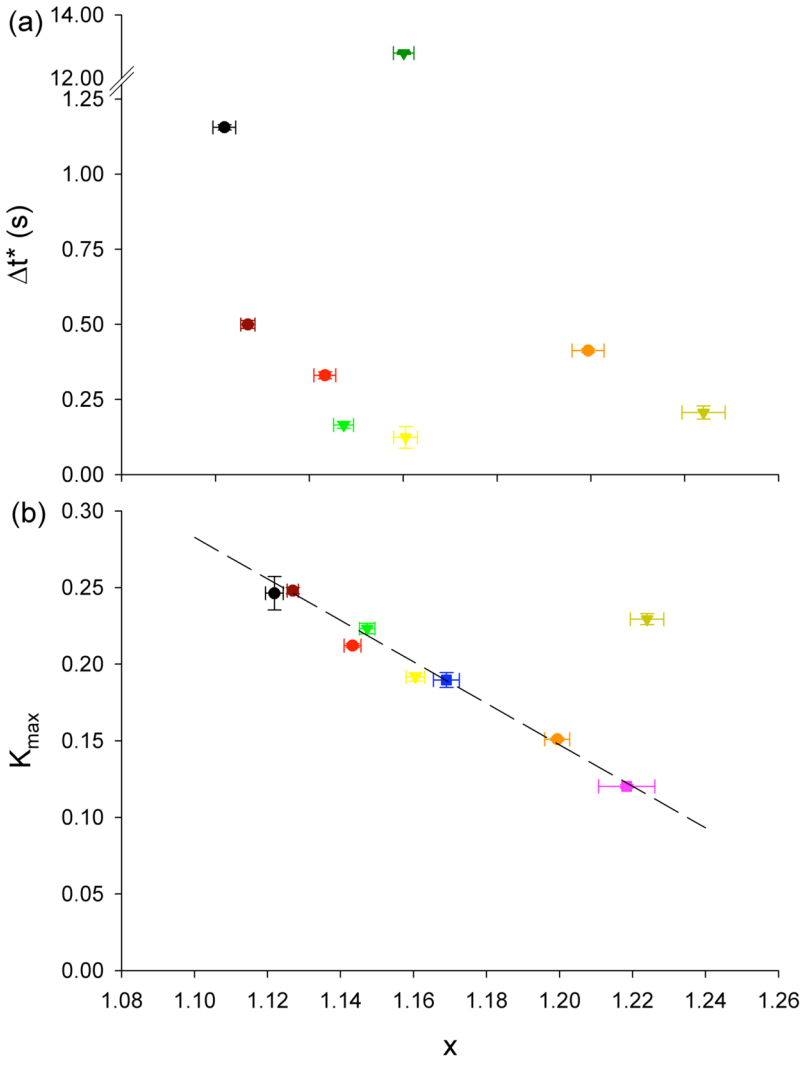

FIG. 4.

(a) Transition time, Δt*, from antipersistent to persistent behaviour *vs.* x. where x-1 is the power-law dependence of g′ upon frequency. (b) Maximum value of K(Δt), K_{max}, as a function of x. Color coding same as Fig. 1 and Fig. 3. K_{max} for ATP depletion could not be calculated, but does not fall within other values. Dotted line is a guide for the eyes.s